Demonstration of Soft–X-Ray Amplification in Nickel-like Ions

B. J. MacGowan, S. Maxon, P. L. Hagelstein,[a] C. J. Keane, R. A. London, D. L. Matthews, M. D. Rosen, J. H. Scofield, and D. A. Whelan

Lawrence Livermore National Laboratory, Livermore, California 94550

(Received 10 August 1987)

We report the first observation of amplification of spontaneous emission at soft x-ray wavelengths by ions in the nickel-like sequence. The ions are created by high-intensity laser irradiation of a thin foil. Gains of order 1 cm^{-1} are observed on $J=0$-1, $4d$-$4p$ transitions in Eu^{35+} at 65.83 and 71.00 Å. There is some evidence for amplification on the analogous lines at 50.26 and 56.09 Å in Yb^{42+}. The pumping mechanism is believed to be electron collisional excitation from the ground state. The scheme should be readily scalable to produce amplification in W^{46+} at 43.15 Å.

PACS numbers: 42.60.By, 32.30.Rj, 32.70.−n, 52.50.Jm

Since the demonstration of an extreme ultraviolet amplifier at 206.3 and 209.6 Å,[1,2] there has been much effort to develop an amplifier to produce significant power at wavelengths below the carbon K absorption edge at 43.76 Å. One motivation is to produce a coherent, monochromatic, high-brightness source suitable for holography of biological specimens in the "water window" between the K edges of carbon and oxygen.[3]

The work of Matthews *et al.*[1] achieved gain on $3p$-$3s$ transitions in neonlike selenium ions produced by intense irradiation of a thin Se foil. The explosion of the foil led to the creation of a plasma which served as the amplifier medium. The dominant line expected to be amplified was the $J=0$-1 transition at 182.4 Å, predicted to be pumped by electron collisional excitation from the ground state.[4] Reference 1 did not observe large gain on the $J=0$-1 line but instead saw gains of order 5 cm^{-1} on $J=2$-1 transitions. The population mechanisms for the $J=2$ levels are more complicated, including contributions by direct collisional excitation, recombination, and cascading from higher energy levels.

The Ne-like Se result has been extrapolated to higher-Z ions. Y^{29+} has shown gain at 155.0 and 157.1 Å while Mo^{32+} has produced a gain of 4 cm^{-1} at 131.0 and 132.7 Å.[5] However, the rapid scaling[6] of laser power required with increased target Z makes Ne-like schemes unsuitable for extrapolation to the water window. The increase in irradiance between Se and Mo was from 5×10^{13} to 4×10^{14} W cm^{-2}. To obtain gain below 43.76 Å would require producing Gd^{54+} with an estimated irradiance in excess of 10^{16} W cm^{-2}. This would be impossible to apply over a long plasma with currently available laser drivers.

The theory of a Ni-like analog to the Ne-like scheme has been discussed previously[7-9] but has lacked an experimental validation. The population inversion necessary for amplification is produced between the $4d$ and $4p$ levels which lie above a $3d^{10}$ closed shell. Figure 1 is a simplified level diagram for Eu^{35+} showing the four $4d$-$4p$ transitions most likely to be amplified. The dominant population mechanism for the $(3d^9_{3/2}4d_{3/2})_0$ level is electron collisional excitation from the ground state. The collision rate is shown in Fig. 1 for an electron density of 2×10^{20} cm^{-3} and electron temperature of 600 eV. This rate is calculated with the multiconfiguration, relativistic, distorted-wave code MCDW.[9] The $J=2$ and $J=1$ $4d$ levels are fed by collisions from the ground state but are also populated by recombination, cascading from higher n states, and feeding from the $4f$ levels. The $4d$-$4p$ population inversion is maintained by the fast $4p$-$3d$ radiative decay, and reduction of this decay rate by trapping will reduce the inversion. A 137-level, time-dependent model for Zn-like, Cu-like, Ni-like, and Co-like Gd has been incorporated in the XRASER kinetics code[10] and the two-dimensional hydrodynamics output from LASNEX[11] used as a basis to predict the expected gains on the four Eu^{35+} transitions shown in Fig. 1. A Gd atomic data file

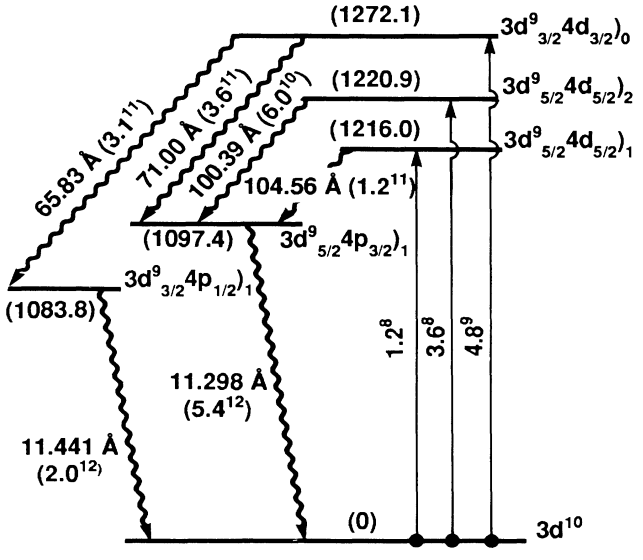

FIG. 1. Simplified level diagram for Eu^{35+} showing the transitions of interest. The collision rates are given for $n_e=2\times10^{20}$ cm^{-3} and $T_e=600$ eV. Level energies (in electronvolts) and spontaneous emission rates are in parentheses.

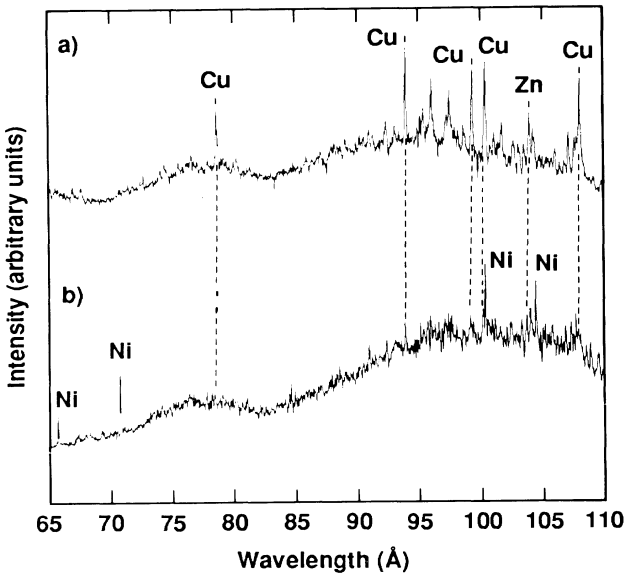

FIG. 2. $4l$-$4l'$ Eu spectra. (a) Off-axis observed spectrum. (b) On-axis observed spectrum.

was used to model Eu ($Z=63$) as early, unsuccessful attempts to fabricate thin-foil targets had centered on Gd ($Z=64$). The model included the effect of trapping of the $4p$-$3d$ transitions. Two types of target foils were used in the experiment, 50-μg-cm^{-2} EuF_2 on 10-μg-cm^{-2} CH and 90-μg-cm^{-2} EuF_2 on 10-μg-cm^{-2} CH. The targets were irradiated with a total of 7×10^{13} W cm^{-2} in two opposing line foci 200 μm wide with a pulse of 1 nsec duration. Simulations[12] of the experiments showed expected gains for both targets of order unity on the four Ni-like lines with the 65.83- and 71.00-Å $J=0$-1 lines predicted to have gains of 0.8 and 1.0 cm^{-1}, respectively. The gain was calculated to appear near the peak of the heating pulse when the electron temperature and density were expected to be 600 eV and 2×10^{20} cm^{-3}, respectively.

Two beams of the Nova laser were used for the experiment; the setup was similar to that described in Ref. 5. The principal diagnostics were grazing-incidence grating spectrometers with microchannel plate detectors capable of being gated in time. Two spectrometers were positioned so as to view the target along the axis of the line focus (the preferred direction for amplification), and a third viewed the target from 45° off axis. The signals from the spectrographs were integrated over time up to 500 ps after the peak of the 0.53-μm Nova pulse, then gated off. Figure 2 shows spectra from a 50-μg-cm^{-2} EuF_2 target. Figure 2(a) is an off-axis spectrum showing the bright optically thick emission from $4l$-$4l'$ transitions in Cu-like and Zn-like Eu which have been identified previously.[13] Figure 2(b) is an on-axis spectrum with Zn- and Cu-like emission but also showing bright emission at 65.83, 71.00, 100.39, and 104.56 Å, identified as previously unobserved $4d$-$4p$ transitions in Ni-like Eu. The line identifications are based on their proximity to calculated values and their behavior as the length of the target is increased. The predicted wavelengths[14] for the lines are shown in Table I. The disagreement with the measured wavelengths of the two shorter-wavelength lines arises from difficulty in calculating the energy of the $J=0$ state due to configuration-interaction contributions. As the two lines share the same upper state, the disagreements with the measured transition energies are similar (0.32 and 0.49 eV). A third, weaker $J=0$-1 transition from the same level (observed at 84.83 Å, on the longest targets) has a similar energy deviation.

Figure 3 shows sections of typical on-axis spectra from targets of different lengths. The $J=0$-1 lines show a nonlinear increase in intensity as the target length is increased, with the 71.00-Å line increasing more rapidly than the 65.83-Å line. Spectra were scanned by a digitizing densitometer and the resultant film density values converted to intensity with a calibration wedge, developed with the data. The intensity of an individual line was then measured by our subtracting out the background continuum level and integrating over the line profile. The results of these measurements are plotted in Fig. 4(a) for the two $J=0$-1 lines and for the $4f^2F_{5/2}$-$4d^2D_{3/2}$ Cu-like transition at 93.84 Å. The data shown are for the 50-μg-cm^{-2} EuF_2 targets. The $J=0$-1 data

TABLE I. Table of calculated and observed wavelength values in angstroms for Ni-like $4d$-$4p$ transitions. The Yb and W $j=0$-1 calculations have been adjusted on the basis of the observed Eu wavelengths.

	Eu^{35+}		Yb^{42+}		W^{46+}
Transition	Theory	Observed	Extrapolated theory	Observed	Extrapolated theory
$(3d^9_{3/2}4d_{3/2})_0$-$(3d^9_{3/2}4p_{1/2})_1$	65.72	65.83 ± 0.03	50.24	50.26 ± 0.05	43.15
$(3d^9_{3/2}4d_{3/2})_0$-$(3d^9_{5/2}4p_{3/2})_1$	70.80	71.00 ± 0.03	56.10	56.09 ± 0.05	49.34
$(3d^9_{3/2}4d_{3/2})_0$-$(3d^9_{3/2}4p_{3/2})_1$	84.62	84.83 ± 0.05	72.04	···	66.39
$(3d^9_{5/2}4d_{5/2})_2$-$(3d^9_{5/2}4p_{3/2})_1$	100.32	100.39 ± 0.03	81.03	···	72.27
$(3d^9_{5/2}4d_{5/2})_1$-$(3d^9_{5/2}4p_{3/2})_1$	104.56	104.56 ± 0.05	84.44	84.40 ± 0.05	75.29

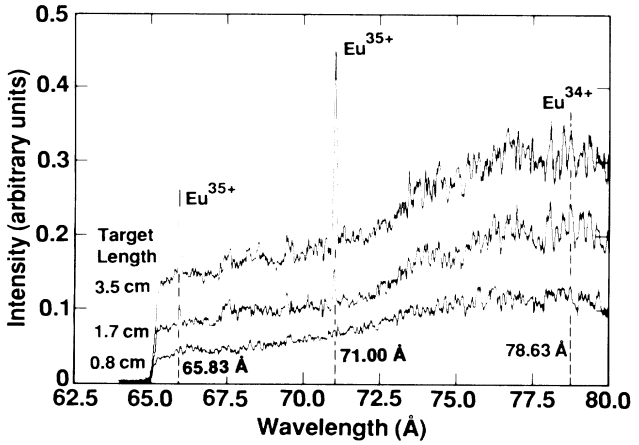

FIG. 3. Details from on-axis spectra in the region near the $J=0$-1 lines of Eu^{35+} for three different target lengths.

have been fitted by the formula

$$I \sim (e^{\alpha l}-1)^{3/2}(\alpha l e^{\alpha l})^{-1/2}, \quad (1)$$

for the output power of a Doppler-broadened, homogeneous, time-independent, distributed source of amplified spontaneous emission[15] of gain coefficient α and length l. The 71.00- and 65.83-Å data were fitted by gains of 1.11 ± 0.12 and 0.61 ± 0.14 cm^{-1}, respectively. The relative sizes of the gains are qualitatively consistent with the relative oscillator strengths[16] of the two lines. The uncertainties in the gains (68% confidence) are calculated on the assumption of an intrinsic error of (15–20)% in the intensity values. The expected plasma conditions would lead to an absorption coefficient of the order of 300 cm^{-1} for the $4f^2F_{5/2}$-$4d^2D_{3/2}$ Cu-like line; the flat scaling of this line with target length is consistent with its being optically thick. Figure 4(b) shows the length behavior of the $J=2$-1 and $J=1$-1 lines. Fits by the small-αl limit of Eq. (1) give $\alpha = 0.08 \pm 0.14$ cm^{-1} for the $J=2$-1 and $\alpha = -0.07 \pm 0.19$ cm^{-1} for the $J=1$-1, essentially linear. The simulated gains were much higher (1.6 and 1.0 cm^{-1}, respectively). In order for the lines to be seen above continuum level there must be a significant emissivity. In the calculation the excited-state population required to give the necessary emissivity also gave high gain. However, a larger population than expected in the $4p$ lower level, as could be produced by additional trapping (which already has a large effect on the $J=2$-1 and $J=1$-1 simulated gains[12]), would destroy the gain while leaving a large emissivity. Such an increase would affect the $J=2$-1 and $J=1$-1 gains more than the $J=0$-1 gains, because of the weighting of the lower-level population by the ratio of the statistical weights in the expression for population inversion. The gains could also be lower than calculated as a result of the difficulty in accurately modeling the multitude of $J=2$ and $J=1$ population mechanisms, or as a result of more refraction by plasma density gradients than is already included in the simulation.[12]

The optical depth of the bremsstrahlung continuum emission at 66 Å is calculated to be less than 0.2 for the longest target. The behavior of the continuum is shown in Fig. 4(b) to be linear, consistent with its being dominated by optically thin emission. The observation of the expected behavior of the continuum and the optically

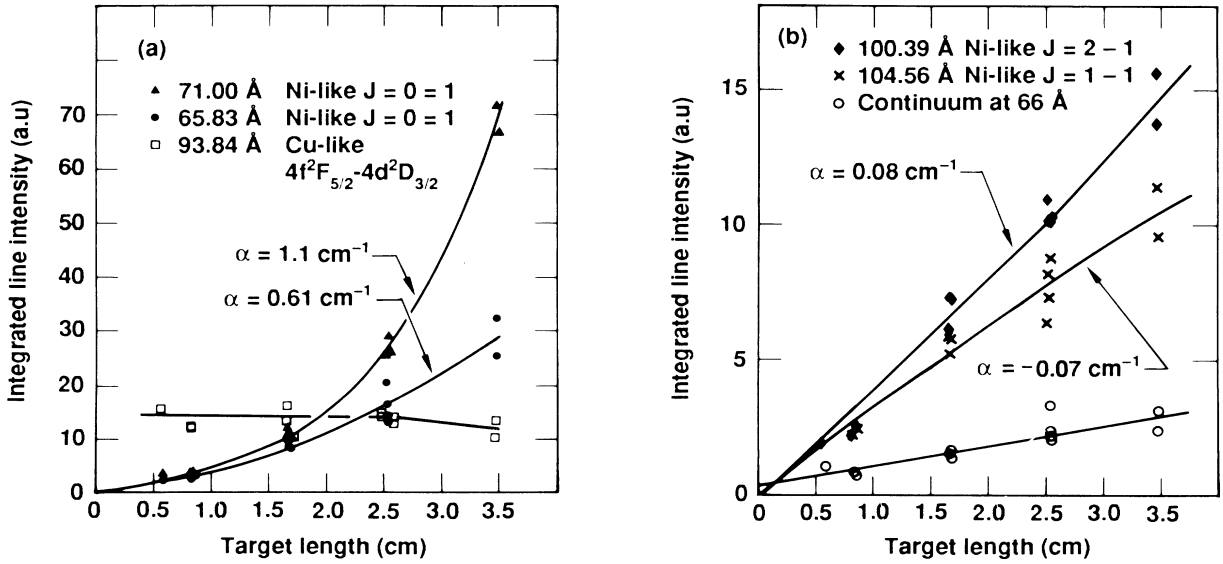

FIG. 4. Intensities as functions of length for five lines and the continuum at 66 Å from the on-axis spectra. The Ni-like line intensities are fitted by Eq. (1). The line through the 93.84-Å data is not a mathematical fit; the continuum is fitted by a straight line.

thick Cu-like line at 93.84 Å verifies that the spectrometers are providing a reliable measurement.

Data for the 90-μg-cm^{-2} EuF_2 targets, analyzed in a similar manner, resulted in gains of 0.60 ± 0.09, 0.24 ± 0.17, 0.01 ± 0.12, and -0.38 ± 0.16 cm^{-1} for the 71.00-, 65.83-, 100.39-, and 104.56-Å lines, respectively. Again the $J=2$-1 and $J=1$-1 gains disagree with calculation and the $J=0$-1 gains are now reduced. The thicker targets would be expected to be hotter, denser, and more ionized,[6] and also to suffer more from trapping of the $4p$-$3d$ transition. All of these changes would affect the gain coefficients.

The extrapolation of the Ni-like scheme to shorter wavelength was explored by our looking at Yb. The targets were 100-μg-cm^{-2} Yb on 10-μg-cm^{-2} CH irradiated at 1.4×10^{14} W cm^{-2} in a 1-ns pulse. Line emissions at 50.26 and 56.09 Å were identified as being the $J=0$-1 transitions in Yb^{42+}. The line at 50.26 Å increases nonlinearly with target length, consistent with its being amplified with a gain of the order of 1 cm^{-1}. The length behavior of the 56.09-Å line is closer to linear. The oscillator strengths are calculated[16] to be 0.075 and 0.061 for the 50.26- and 56.09-Å lines, respectively, and so the shorter-wavelength line would be expected to have slightly more gain. Table I shows the observed and calculated wavelengths of all the Ni-like lines seen to date. The calculated wavelengths for tungsten are also given, demonstrating the scaling of the shorter wavelength $J=0$-1 line to below the carbon K edge.

In conclusion, we have demonstrated that gain can be produced in a laser-heated exploding foil plasma of Ni-like ions. This demonstration now opens the way for extrapolation of present-day, relatively long-wavelength extreme ultraviolet lasers[1,5] to a domain where they are truly soft x rays. The scaling of the scheme to shorter wavelength is promising, as indicated by the results with Yb. We predict that an exploding-foil amplifier of tungsten will produce gain at 43.15 Å with heating pulse intensities of approximately 4×10^{14} W cm^{-2}.

The authors gratefully acknowledge contributions from P. Bell, S. Brown, A. Burnham, E. M. Campbell, J. Cox, G. Jameson, G. Hermes, D. Nilson, G. Powers, and L. Wettstein of Lawrence Livermore National Laboratory and G. Steele and W. Sharp of Luxel Corporation. This work was performed under the auspices of the U. S. Department of Energy by the Lawrence Livermore National Laboratory under Contract No. W-7405-ENG-48.

---

[a]Present address: Department of Electrical Engineering, Massachusetts Institute of Technology, Cambridge, MA 02139.

[1]D. L. Matthews *et al.*, Phys. Rev. Lett. **54**, 110 (1985).

[2]M. D. Rosen *et al.*, Phys. Rev. Lett. **54**, 106 (1985).

[3]B. L. Henke, in *Encyclopedia of Microscopy,* edited by G. L. Clark (Reinhold, New York, 1961), p. 675.

[4]A. N. Zherikhin *et al.*, Kvantovaya Elektron. (Moscow) **3**, 152 (1976) [Sov. J. Quantum Electron. **6**, 82 (1976)]; A. V. Vinogradov and V. N. Shylaptsev, Kvantovaya Elektron. (Moscow) **10**, 2325 (1983) [Sov. J. Quantum Electron. **13**, 1511 (1983)], and references therein; P. L. Hagelstein, Ph.D. thesis, University of California, Lawrence Livermore National Laboratory Report No. UCRL-53100, 1981 (unpublished); U. Feldman *et al.*, J. Appl. Phys. **54**, 2188 (1983), and **56**, 2475 (1984).

[5]B. J. MacGowan *et al.*, J. Appl. Phys. **61**, 5243 (1987).

[6]R. A. London and M. D. Rosen, Phys. Fluids **29**, 3813 (1986).

[7]S. Maxon *et al.*, J. Appl. Phys. **57**, 971 (1985).

[8]S. Maxon *et al.*, J. Appl. Phys. **59**, 239 (1986).

[9]P. L. Hagelstein, Phys. Rev. A **34**, 874 (1986).

[10]P. L. Hagelstein, Plasma Phys. **25**, 1345 (1983).

[11]G. B. Zimmerman and W. L. Kruer, Comments Plasma Phys. Controlled Fusion **2**, 85 (1975).

[12]S. Maxon *et al.*, to be published.

[13]J. Reader and G. Luther, Phys. Rev. Lett. **45**, 609 (1980); N. Acquista and J. Reader, J. Opt. Soc. Am. B **1**, 649 (1984); G. A. Doschek *et al.*, to be published.

[14]M. H. Chen and J. H. Scofield, private communication; calculation using Grant's MCDF code [I. P. Grant *et al.*, Comput. Phys. Commun. **21**, 207 (1980)].

[15]G. J. Linford *et al.*, Appl. Opt. **12**, 379 (1974).

[16]Oscillator strengths calculated from the relativistic configuration-interaction calculation YODA. P. L. Hagelstein and R. K. Jung, unpublished.